

## Supplemental Material

In the following, we provide details of the Casimir sensing scheme presented in the main text. In Sec. I, we address the effect of quantum vacuum potentials on a quantum emitter and explain how the modified energy level shifts and decay rates of a two level system close to a surface can be calculated. In Sec. II, we derive the effective (linear) Casimir coupling Hamiltonian in the weak driving limit and in in Sec III, we provide a detailed description of the optical read-out of the Casimir-potential induced level shifts and show how the motion of a membrane can be monitored using coherent light. Throughout the Supplemental Material, we use  $\hbar = 1$ .

### I. CASIMIR-EFFECT FOR QUANTUM EMITTERS

The high sensitivity of the proposed sensing scheme is due to the large energy shifts that vacuum forces can induce in a quantum emitter close to a dielectric surface. In the following, we explain how these level shifts can be calculated. The general expressions for the ground and excited state shifts  $\delta\omega_g$  and  $\delta\omega_e$  of an effective isotropic two-level emitter are given by [S1]

$$\delta\omega_g(\mathbf{r}) = \frac{3c\Gamma_0}{\omega_{eg}^2} \int_0^\infty du \frac{u^2}{\omega_{eg}^2 + u^2} \text{Tr} G(\mathbf{r}, \mathbf{r}, iu),$$

$$\delta\omega_e(\mathbf{r}) = -\delta\omega_g(\mathbf{r}) - \frac{\Gamma_0\pi c}{\omega_{eg}} \text{Tr Re} G(\mathbf{r}, \mathbf{r}, \omega_{eg}),$$

where  $G(\mathbf{r}, \mathbf{r}, \omega_{eg})$  is the classical (dyadic) electromagnetic Green's function. As described in the main text, the ground-state shift arises from excitation non-conserving terms in the atom-field interaction Hamiltonian involving the virtual emission and re-absorption of a photon. This contribution is most easily evaluated by rotating the arising integral to complex frequencies  $\omega = iu$ . The excited-state shift contains one term ( $-\delta\omega_g(\mathbf{r})$ ) that arises from virtual emission and re-absorption of off-resonant photons from the excited state, and an additional term coming from the emission of a real photon (proportional to the Green's function at the resonance frequency  $\omega_{eg}$ ). Similarly, the spontaneous emission rate of this real photon can be modified in the presence of a dielectric surface [S1],

$$\Gamma(\mathbf{r}) = \Gamma_0 + \frac{2\Gamma_0\pi c}{\omega_{eg}} \text{Tr Im} G(\mathbf{r}, \mathbf{r}, \omega_{eg}).$$

The Green's function satisfies the equation

$$\left[ (\nabla \times \nabla \times) - \frac{\omega^2}{c^2} \epsilon(\mathbf{r}, \omega) \right] G(\mathbf{r}, \mathbf{r}', \omega) = \delta(\mathbf{r} - \mathbf{r}') \otimes I.$$

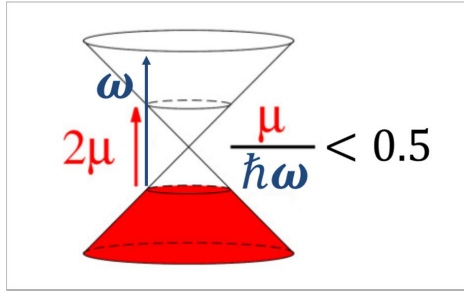
We approximate the Green's function of a suspended graphene mechanical resonator by that of an infinite graphene sheet, as the latter has an exact solution. This approximation is well-justified given that the regime of interest is one where the emitter sits at much closer distances  $d$  to the graphene than the lateral size of the sheet  $L$ ,  $d \ll L$ .

To be specific, we consider an infinite interface between vacuum and a dielectric surface located at  $z = 0$ . The Green's function generally consists of an unimportant free term and a reflected component, the latter of which gives rise to position dependence in the level shifts and decay rates. Physically, this term describes the interaction of the emitter with its own field reflected from the surface. For distances  $z > 0$  (on the vacuum side), the trace of this reflected component is

$$\text{Tr} G(z, z, \omega) = \frac{ic^2}{4\pi\omega^2} \int_0^\infty dk_\parallel \frac{k_\parallel}{k_\perp} e^{2ik_\perp z} \left( \frac{\omega^2}{c^2} r_s + (k_\parallel^2 - k_\perp^2) r_p \right).$$

Here  $k_\parallel$  and  $k_\perp$  are the parallel and perpendicular wavevector components, with  $k_\perp = \sqrt{(\omega/c)^2 - k_\parallel^2}$ . The Fresnel reflection coefficients for  $s$  and  $p$ -polarized waves in the case of graphene are given by  $r_p = \frac{k_\perp \sigma}{k_\perp \sigma + 2\epsilon_0 \omega}$  and  $r_s = -\frac{\mu_0 \sigma \omega}{2k_\perp + \mu_0 \sigma \omega}$  and depend on the conductivity  $\sigma$  [S2]. The conductivity of graphene [S3, S4] is given by

$$\sigma(\omega) = \frac{e^2 \mu}{\pi} \frac{i}{\omega + i\gamma_g} + \frac{e^2}{4} \left[ \Theta(\omega - 2\mu) + \frac{i}{\pi} \log \left| \frac{\omega - 2\mu}{\omega + 2\mu} \right| \right], \quad (\text{S.1})$$



Supplementary figure S.1: Band structure of doped graphene with Fermi level  $\mu$ . Occupied electronic states are shown in red. If the energy of an incoming photon  $\hbar\omega$  exceeds  $2\mu$ , it can induce a transition from the lower band to the upper one.

where  $\mu$  is the Fermi energy and  $\gamma_g$  is a phenomenological parameter characterizing intraband losses. For our numerical simulations, we use  $\omega_0/\gamma_g = 10^3$ .

The conductivity of graphene has two physically distinct components. The first term on the right, proportional to  $\mu$ , corresponds to that of a free-electron gas (i.e., a Drude metal) and describes the response of carriers within a single band of graphene. The second term (in brackets) describes the effect of optically-induced transitions between the different bands of graphene. It consists of a real term (characterizing absorption) proportional to a step function, which turns on for frequencies  $\omega > 2\mu$ , due to the availability of electron-hole transitions at these frequencies (see Fig. S.1). The imaginary term describes dispersive effects associated with a step-function absorption profile, as required by Kramers-Kronig relations.

In the regime  $\omega \lesssim 2\mu$ , interband effects can be neglected and graphene behaves like a Drude metal. In this case, graphene supports guided surface plasmon modes, like any thin conducting film [S5]. The plasmonic wavelength-frequency dispersion relation is given by  $\lambda_{sp}/\lambda_0 = 2\alpha(\mu/\omega)$ , where  $\alpha$  is the fine-structure constant and  $\lambda_0 = 2\pi c/\omega$  is the free-space wavelength [S3]. An emitter within a distance  $d \approx \lambda_{sp}$  of the surface experiences strong spontaneous emission into the plasmon modes.

## II. LINEARIZATION OF THE CASIMIR COUPLING HAMILTONIAN

In the following, we explain how the Casimir coupling Hamiltonian can be linearized in the the weak driving limit and outline how the effective light-membrane interaction Hamiltonian (Eq. (3) in the main text) is obtained.

The dynamics of the membrane and the emitter is governed by

$$\begin{aligned}\dot{\rho} &= -i[H, \rho] + \Gamma \mathcal{D}_{\sigma_-}(\rho), \\ H &= \frac{\Delta}{2}\sigma_z + \frac{\Omega}{2}\sigma_x + \omega_M a_M^\dagger a_M + g x_M \sigma_z, \\ \mathcal{D}_{\sigma_-}(\rho) &= \sigma_- \rho \sigma_+ - \frac{1}{2}\sigma_+ \sigma_- \rho - \frac{1}{2}\rho \sigma_+ \sigma_-, \end{aligned}$$

and leads to modified mechanical and emitter properties such as a  $\langle \sigma_z \rangle$ -dependent displacement of the steady state value of the mechanical position  $\langle x_M \rangle_\infty$  and a renormalized detuning  $\Delta \rightarrow \Delta + g \langle x_M \rangle_\infty$ . The differential equation above can be decomposed into an entangling part given by the coupling Hamiltonian  $H_{\text{int}} = g x_M \sigma_z$ , which creates correlations between the emitter and the light field, and a separable part

$$\mathcal{L}_0(\rho) = -i \left[ \frac{\Delta}{2}\sigma_z + \frac{\Omega}{2}\sigma_x, \rho \right] + \Gamma \mathcal{D}_{\sigma_-}(\rho).$$

We consider the case  $\Gamma \gg g$ , where the two level system reaches its steady state on a time scale which is fast compared to the timescale on which the exchange of information between the emitter and the membrane take place. The steady state of  $\mathcal{L}_0(\rho)$ ,

$$\rho_0 = \begin{pmatrix} \frac{\Omega^2}{\frac{\Omega^2}{2} + \Delta^2 + \frac{\Gamma^2}{4}} & \frac{\Omega}{2} \frac{\langle \sigma_z \rangle_\infty}{\Delta + i\frac{\Gamma}{2}} \\ \frac{\Omega}{2} \frac{\langle \sigma_z \rangle_\infty}{\Delta - i\frac{\Gamma}{2}} & \frac{\Omega^2 + \Delta^2 + \frac{\Gamma^2}{4}}{\frac{\Omega^2}{2} + \Delta^2 + \frac{\Gamma^2}{4}} \end{pmatrix},$$

with

$$\langle \sigma_z \rangle_\infty = -1 + \frac{\epsilon}{2} + \mathcal{O}(\epsilon^2),$$

is a pure state in the weak driving limit, i.e. up to  $\mathcal{O}(\epsilon)$ , where  $\epsilon = \frac{\Omega^2}{\Delta^2 + (\Gamma/2)^2}$ . This allows us to introduce a unitary transformation  $R$ , which rotates the ground state of the emitter into the steady state of  $\mathcal{L}_0$ ,  $R^\dagger|g\rangle\langle g|R = \rho_0$ . We are interested in deviations of relevant observables from their steady state mean value and describe the interaction between the emitter and the membrane therefore in a rotated and displaced picture where

$$H_{\text{int}} = -g \left(1 - \frac{\epsilon}{8}\right) \frac{\Omega}{\Delta^2 + \frac{\Gamma^2}{4}} \left( \Delta \sigma_x + \frac{\Gamma}{2} \sigma_y \right) x_M + \mathcal{O}(\epsilon^2).$$

Since the emitter explores only a small region on the surface of the Bloch sphere around  $\rho_0$ , this region can be approximated by a plane and the two level system can be treated as harmonic oscillator with quadratures

$$x_E = \frac{\bar{\alpha} \sigma_y + \bar{\beta} \sigma_x}{\sqrt{2\epsilon |\langle \sigma_z \rangle_\infty|}}, \quad p_E = \frac{-\bar{\beta} \sigma_y + \bar{\alpha} \sigma_x}{\sqrt{2\epsilon |\langle \sigma_z \rangle_\infty|}},$$

such that

$$H_{\text{int}} = \bar{g} \sqrt{\epsilon} x_M x_E, \tag{S.2}$$

to first order in  $\epsilon$ , where

$$\bar{g} = -g\sqrt{2} \left(1 - \frac{3}{8}\epsilon\right), \quad \bar{\alpha} = \frac{\Omega \frac{\Gamma}{2}}{\Delta^2 + \frac{\Gamma^2}{4}}, \quad \bar{\beta} = \frac{\Omega \Delta}{\Delta^2 + \frac{\Gamma^2}{4}}. \tag{S.3}$$

The emitter interacts with the membrane through Eq. (S.2) and with the light-field via the standard optical Bloch equations. For  $\epsilon \ll 1$ , the emitter can be adiabatically eliminated, which yields an effective interaction between the membrane and the light field

$$H_{\text{ML}} = \kappa x_M p_L, \tag{S.4}$$

where  $\kappa = \bar{g} \sqrt{\epsilon \Gamma_{\text{det}}} / \Gamma$  and  $p_L$  is the light field quadrature, which couples to  $x_E$  (see Sec. III). A detailed derivation of the corresponding equations of motion is provided in Sec. III A. Eq. (S.4) describes the mapping of displacements of the membrane  $x_M$  to phase shifts on the scattered light field that are described by the quadratures  $x_L$  and  $p_L$  (see below). These phase shift can be very efficiently measured against a reference beam using homodyne detection [S6].

### III. READ-OUT SCHEME

This section is devoted to the read-out of the Casimir potential induced level shifts using coherent light fields. In Sec. III A, the effective emitter-mediated time evolution of the membrane and the light field is derived and in Sec. III B we explain how the conditional variance of the membrane can be calculated if the scattered light field is measured by homodyne detection. Throughout this part of the Supplemental Material, we will use dimensionless mechanical quadratures  $x_m = x_M \sqrt{\omega_M m}$ ,  $p_m = p_M \sqrt{1/(\omega_M m)}$  (as above, we use  $\hbar = 1$ ). With this notation, the Casimir coupling Hamiltonian derived in Sec. II is given by

$$H_{\text{int}} = \bar{g}_m \sqrt{\epsilon} x_E x_m, \quad \bar{g}_m = \bar{g} (m \omega_M)^{-\frac{1}{2}}. \tag{S.5}$$

#### A. Time evolution of the emitter, the membrane and the light field

In this section, we derive the input-output relations for the light field and the membrane in the weak driving limit by adiabatically eliminating the emitter.

### 1. Light-emitter interaction and adiabatic elimination of the excited state

In the following, we consider the evolution of the light field and the emitter. As explained above, the properties of the emitter are read out by applying a laser beam and detecting the phase shift that has been acquired by the light field. The phase shift on the light field are here described in terms of the light field quadratures  $x_L$  and  $p_L$ . They describe the in-phase and out-of-phase component of the light with respect to some reference laser field [S6]. The former corresponds to the sine component (with a phase difference of  $\phi = 0$  with respect to the reference beam) of the electromagnetic field. The latter corresponds to the cosine component (with a phase difference of  $\phi = \pi/2$ ). We use here spatially localized light modes  $x_L(t), p_L(t)$  with commutation relations  $[x_L(t), p_L(t')] = i\delta(t - t')$ . The light mode corresponding to  $x_L(t), p_L(t)$  interacts with the emitter at time  $t$  through the dipole interaction, resulting in the transformation

$$\begin{pmatrix} x_L^{\text{out}}(t) \\ p_L^{\text{out}}(t) \end{pmatrix} = \begin{pmatrix} x_L^{\text{in}}(t) \\ p_L^{\text{in}}(t) \end{pmatrix} + \sqrt{\Gamma_{\text{det}}} \begin{pmatrix} -p_E(t) \\ x_E(t) \end{pmatrix}, \quad (\text{S.6})$$

where the superscripts "in" and "out" label the variables before and after the interaction. The emitter is subject to three different types of interactions. It couples to the light field and interacts with the membrane through the Casimir potential, as described by Eq. (S.5). Moreover, the emitter can scatter light into channels which are not measured. The latter is taken into account by introducing noise modes  $x_N(t), p_N(t)$  with  $[x_N(t), p_N(t')] = i\delta(t - t')$  such that

$$\begin{pmatrix} \dot{x}_E(t) \\ \dot{p}_E(t) \end{pmatrix} = \sqrt{\Gamma_{\text{det}}} \begin{pmatrix} -p_L^{\text{in}}(t) \\ x_L^{\text{in}}(t) \end{pmatrix} + \sqrt{\Gamma_N} \begin{pmatrix} -p_N^{\text{in}}(t) \\ x_N^{\text{in}}(t) \end{pmatrix} - \bar{g}_m \sqrt{\epsilon} \begin{pmatrix} 0 \\ x_m(t) \end{pmatrix} - \frac{\Gamma}{2} \begin{pmatrix} x_E(t) \\ p_E(t) \end{pmatrix},$$

where  $\Gamma = \Gamma_{\text{det}} + \Gamma_N$ . In the weak driving limit, where  $\epsilon = \frac{\Omega^2}{\Delta^2 + \frac{\Gamma^2}{4}} \ll 1$ , the population of the excited state is negligible and the emitter can be adiabatically eliminated. For  $\epsilon \ll 1$  and  $\omega_M \ll \Gamma$ ,

$$\begin{pmatrix} x_E(t) \\ p_E(t) \end{pmatrix} = \frac{2\sqrt{\Gamma_{\text{det}}}}{\Gamma} \begin{pmatrix} -p_L^{\text{in}}(t) \\ x_L^{\text{in}}(t) \end{pmatrix} + \frac{2\sqrt{\Gamma_N}}{\Gamma} \begin{pmatrix} -p_N^{\text{in}}(t) \\ x_N^{\text{in}}(t) \end{pmatrix} - \frac{2\bar{g}_m \sqrt{\epsilon}}{\Gamma} \begin{pmatrix} 0 \\ x_m(t) \end{pmatrix}. \quad (\text{S.7})$$

By inserting this expression into the evolution equation for the membrane and the light field, effective input-output relations for the mechanical and the photonic system can be obtained, which do not include the emitter any more.

### 2. Effective time evolution of the membrane and the light field

The membrane evolves under the Hamiltonian  $H_{\text{membrane}} = \frac{\omega_M}{2}(x_m^2 + p_m^2) + \bar{g}_m \sqrt{\epsilon} x_E x_m$  and is subject to mechanical damping. We consider here two different damping models and analyze the case of symmetric damping when position and momentum are damped with equal rates  $\gamma_x = \gamma_p = \gamma/2$ , and pure momentum damping  $\gamma_x = 0, \gamma_p = \gamma$ . In the case of symmetric damping, the time evolution of the membrane is given by

$$\begin{pmatrix} \dot{x}_m(t) \\ \dot{p}_m(t) \end{pmatrix}_{\text{sym}} = \begin{pmatrix} -\frac{\gamma}{2} & \omega_M \\ -\omega_M & -\frac{\gamma}{2} \end{pmatrix} \begin{pmatrix} x_m(t) \\ p_m(t) \end{pmatrix} + \sqrt{\gamma} \begin{pmatrix} f_{x,\text{sym}}^{\text{in}}(t) \\ f_{p,\text{sym}}^{\text{in}}(t) \end{pmatrix} - \bar{g}_m \sqrt{\epsilon} \begin{pmatrix} 0 \\ x_E(t) \end{pmatrix}, \quad (\text{S.8})$$

where  $\gamma$  is the mechanical decay rate and  $f_{x,\text{sym}}^{\text{in}}, f_{p,\text{sym}}^{\text{in}}$  are the associated Langevin noise operators with  $[f_{x,\text{sym}}^{\text{in}}(t), f_{p,\text{sym}}^{\text{in}}(t')] = i\delta(t - t')$ . The noise correlation functions are given by  $\langle f_{x,\text{sym}}^{\text{in}}(t) f_{x,\text{sym}}^{\text{in}}(t') \rangle = \langle f_{p,\text{sym}}^{\text{in}}(t) f_{p,\text{sym}}^{\text{in}}(t') \rangle = \delta(t - t')(2n_{\text{th}} + 1)$ , where  $n_{\text{th}}$  is the thermal occupation number and is given by  $n_{\text{th}} = k_B T_{\text{bath}} / \omega_m$ .  $k_B$  is the Boltzmann constant and  $T_{\text{bath}}$  is the temperature of the bath of the membrane.

In the following, we derive the effective evolution for pure momentum damping. The symmetric case can be treated in an analogous fashion. Physically, many known damping mechanisms lead to momentum- rather than position damping. However, the quantized description of pure momentum damping is a complicated problem which is for example addressed in the Caldeira-Leggett model [S7, S8] and involves non-Markovian noise operators. We use here a simplified Markovian model, which can be understood as the quantum analogue of classical Brownian motion [S9, S10]. A direct Markovian quantum analogue of the equations describing classical Brownian motion does in general not preserve the positivity of the density matrix describing the quantum state [S11]. This can be corrected by adding an appropriate noise term in the evolution of  $x_m(t)$  [S12, S13]. The corresponding quantum Langevin equations for the mechanical quadratures are given by

$$\begin{pmatrix} \dot{x}_m(t) \\ \dot{p}_m(t) \end{pmatrix} = \begin{pmatrix} 0 & \omega_M \\ -\omega_M & -\gamma \end{pmatrix} \begin{pmatrix} x_m(t) \\ p_m(t) \end{pmatrix} + \sqrt{\gamma} \begin{pmatrix} f_x^{\text{in}}(t) \\ f_p^{\text{in}}(t) \end{pmatrix} - \bar{g}_m \sqrt{\epsilon} \begin{pmatrix} 0 \\ x_E(t) \end{pmatrix},$$

with  $[f_x^{\text{in}}(t), f_p^{\text{in}}(t')] = i\delta(t - t')$  and noise correlation functions  $\langle f_x^{\text{in}}(t)f_x^{\text{in}}(t') \rangle = \delta(t - t')(2n_{\text{th}} + 1)^{-1}$ ,  $\langle f_p^{\text{in}}(t)f_p^{\text{in}}(t') \rangle = \delta(t - t')(2n_{\text{th}} + 1)$  [S12, S13].

We consider now the time evolution of the membrane in the interaction picture with respect to the free mechanical Hamiltonian  $H_M = \frac{\omega_M}{2}(x_m^2 + p_m^2)$ , i.e. in a co-rotating frame. The corresponding transformed mechanical variables are given by

$$\begin{pmatrix} \tilde{x}_m(t) \\ \tilde{p}_m(t) \end{pmatrix} = \begin{pmatrix} \cos(\omega_M t) & -\sin(\omega_M t) \\ \sin(\omega_M t) & \cos(\omega_M t) \end{pmatrix} \begin{pmatrix} x_m(t) \\ p_m(t) \end{pmatrix} \quad (\text{S.9})$$

and evolve according to

$$\begin{aligned} \begin{pmatrix} \dot{\tilde{x}}_m(t) \\ \dot{\tilde{p}}_m(t) \end{pmatrix} &= \gamma_R \begin{pmatrix} \tilde{x}_m(t) \\ \tilde{p}_m(t) \end{pmatrix} + \sqrt{\gamma} \begin{pmatrix} \cos(\omega_M t)f_x^{\text{in}}(t) - \sin(\omega_M t)f_p^{\text{in}}(t) \\ \sin(\omega_M t)f_x^{\text{in}}(t) + \cos(\omega_M t)f_p^{\text{in}}(t) \end{pmatrix} \\ &+ \frac{2\bar{g}_M\sqrt{\epsilon\Gamma_{\text{det}}}}{\Gamma} \begin{pmatrix} -\sin(\omega_M t) \\ \cos(\omega_M t) \end{pmatrix} p_L^{\text{in}}(t) + \frac{2\bar{g}_M\sqrt{\epsilon\Gamma_{\text{N}}}}{\Gamma} \begin{pmatrix} -\sin(\omega_M t) \\ \cos(\omega_M t) \end{pmatrix} p_N^{\text{in}}(t), \end{aligned} \quad (\text{S.10})$$

where

$$\gamma_R = \gamma \begin{pmatrix} -\sin^2(\omega_m t) & \cos(\omega_m t)\sin(\omega_m t) \\ \cos(\omega_m t)\sin(\omega_m t) & -\cos^2(\omega_m t) \end{pmatrix}.$$

The equations for the evolution of the light field quadratures read

$$\begin{pmatrix} x_L^{\text{out}}(t) \\ p_L^{\text{out}}(t) \end{pmatrix} = \frac{2\bar{g}_m\sqrt{\epsilon\Gamma_{\text{det}}}}{\Gamma} \begin{pmatrix} \cos(\omega_M t)\tilde{x}_m(t) + \sin(\omega_M t)\tilde{p}_m(t) \\ 0 \end{pmatrix} + \left(1 - \frac{2\Gamma_{\text{det}}}{\Gamma}\right) \begin{pmatrix} x_L^{\text{in}}(t) \\ p_L^{\text{in}}(t) \end{pmatrix} - \frac{2\sqrt{\Gamma_{\text{det}}\Gamma_{\text{N}}}}{\Gamma} \begin{pmatrix} x_N^{\text{in}}(t) \\ p_N^{\text{in}}(t) \end{pmatrix}, \quad (\text{S.11})$$

where Eq. (S.6), Eq. (S.7) and Eq. (S.9) have been used. The time evolution equations for the mechanical and light-field variables Eq. (S.10) and Eq. (S.11) correspond to an effective interaction between the membrane and light,  $H_{\text{ML}} = \kappa x_M p_L(t)$  with effective coupling rate  $\kappa = 2\bar{g}\sqrt{\epsilon\Gamma_{\text{det}}}/\Gamma$ .

## B. Calculation of the conditional variance

Eq. (S.11) shows that the mechanical position is mapped to the  $x$ -quadrature of the light field and can accordingly be read-out by monitoring  $x_L$ . As discussed in the following, continuous measurements of  $x_L$  lead to a reduced conditional variance of the position of the membrane.

The term conditional variance refers to the variance that is obtained if the measurement results are known. The term unconditional variance describes the case where the light field is not measured or if the measurement results are not taken into account. In the setting considered here, the conditional variance of the atomic position  $V_x$  can be reduced below  $x_{\text{ZPM}}^2$ , while the unconditional state does not exhibit squeezing. This is due to the fact that the measurements on the light field yield probabilistic outcomes which result in random displacements of the mechanical state in phase space.

In the following, we explain how the conditional variance can be calculated [S14]. For convenience, we discretize time using infinitesimally short time intervals of duration  $\tau \ll \omega_M^{-1}$ ,  $\kappa^{-2}$ ,  $(\gamma \cdot n_{\text{th}})^{-1}$  and discretized light modes  $x_{L,n}^{\text{in}} = \sqrt{\tau}x_L^{\text{in}}(n\tau)$ ,  $p_{L,n}^{\text{in}} = \sqrt{\tau}p_L^{\text{in}}(n\tau)$ .

The light-membrane interaction discussed above leads to an entangled state between the membrane and the light. As outlined above, measurement on the latter allow one to infer information of the former such that a squeezed state is generated. More specifically, for each time step, a light mode in vacuum  $|0\rangle_n$  couples to the membrane in state  $|\Psi_M(n\tau)\rangle$  through the interaction Hamiltonian  $H_{\text{ML}}$ . The subsequent measurement yields outcome  $o_n$  with probability  $p_n$ . In this case, we obtain the conditional state of the membrane  $|\Psi_M([n+1]\tau)\rangle = \frac{1}{\sqrt{p_n}} \langle o_n | e^{-iH_{\text{ML}}\tau} | 0 \rangle_n |\Psi_M(n\tau)\rangle$  and the corresponding unconditional state is given by  $\rho([n+1]\tau) = \sum_n M_n \rho(n\tau) M_n^\dagger$ , where  $M_n = {}_n\langle o_n | e^{-iH_{\text{ML}}\tau} | 0 \rangle_n$ .

This process can be conveniently described in terms of covariance matrices using the Gaussian formalism [S15, S16]. The covariance matrix of a continuous variable system with  $m$  modes that are each described by the quadratures  $x$  and  $p$  is given by  $\Gamma_{ij} = \langle \{ \langle R_i - \langle R_i \rangle, R_j - \langle R_j \rangle \} \rangle_+$ , where  $\{\cdot, \cdot\}$  is the anticommutator and  $\mathbf{R} = (x_1, p_1, \dots, x_m, p_m)^T$ . The covariance matrix of a thermal state is for example given by  $\Gamma_{\text{th}} = (2n_{\text{th}} + 1) \cdot \mathbb{1}$ . Unitary time evolutions  $\mathbf{R}(t) = S(t)\mathbf{R}^{\text{in}}$  can be parametrized by a time evolution matrix  $S$  such that  $\Gamma(t) = S(t)\Gamma^{\text{in}}S(t)^T$ . Using this

notation, the time evolution of the membrane and the light field given by Eq. (S.11) and Eq. (S.10) can be cast in the form  $\Gamma([n+1]\tau) = S(n\tau)\Gamma(n\tau)S^T(n\tau)$ .  $\Gamma([n+1]\tau)$  is here a  $8 \times 8$  square matrix corresponding to  $\mathbf{R}(n\tau) = (x_m(n\tau), p_m(n\tau), x_{L,n}, p_{L,n}, x_{N,n}, p_{N,n}, f_{x,n}, f_{p,n})^T$ . The update of the mechanical state through the measurement of the light [S15] can be calculated by considering the  $4 \times 4$  block of this matrix  $\Gamma_{ML}$  that corresponds to the mechanical and photonic modes

$$\Gamma_{ML} = \begin{pmatrix} \Gamma_M & \Gamma_{\text{coh}} \\ \Gamma_{\text{coh}}^T & \Gamma_L \end{pmatrix},$$

and using the formula

$$\Gamma'_M = \Gamma_M - \Gamma_{\text{coh}}(\Gamma_L + \tilde{\gamma}_L)^{-1}\Gamma_{\text{coh}}^T. \quad (\text{S.12})$$

$\Gamma'_M$  is the updated  $2 \times 2$  matrix, which describes the conditional mechanical state after the measurement, and

$$\tilde{\gamma}_L = \begin{pmatrix} r^{-1} & 0 \\ 0 & r \end{pmatrix}$$

is the covariance matrix of the state onto which the photonic mode is projected. A perfect measurement of  $x_L$  corresponds to  $r \rightarrow \infty$ .

For example, if the initial state of the mechanical system is a thermal state and the dynamics is solely governed by the interaction Hamiltonian  $H_{ML}$  (which is the case in the short time limit for perfect detection), Eq. (S.12) yields directly

$$\dot{V}_x(t) = -\kappa^2 V_x^2(t), \quad \dot{V}_p(t) = \kappa^2,$$

such that

$$V_x(t) = \frac{1}{(V_x^{\text{in}})^{-1} + \kappa^2 t}, \quad V_p(t) = V_p^{\text{in}} + \kappa^2 t.$$

This underlying mechanism which leads to a squeezing in the mechanical  $x$ -quadrature and an antisqueezing in  $p_m$  is complicated by the effects of imperfect detection, the coupling to a thermal bath and the rotation in phase space [S17]. We consider here the measurement process in the rotating frame, since the co-rotating variables  $\tilde{x}_m$  and  $\tilde{p}_m$  are the relevant observables that can be accessed typically. Since the interaction Hamiltonian facilitates a mapping of  $x_m$  onto  $x_L$ ,  $\tilde{x}_m$  and  $\tilde{p}_m$  are mapped and squeezed alternately at a frequency  $\omega_M$ , which gives rise to the oscillations in Fig. 4b in the main text. In the non-rotating frame, the conditional variance of  $x_m$  decreases quickly during a short time interval and reaches then a stationary value with constant squeezing.

- 
- [S1] S. Y. Buhmann, and D.-G. Welsch, Prog. Quantum Electron. **31**, 51 (2007).  
[S2] L. A. Falkovsky, J. Phys.: Conf. Ser. **129** 012004 (2008).  
[S3] B. Wunsch, T. Stauber, F. Sols, and F. Guinea, New J. Phys. **8**, 318 (2006).  
[S4] T. Stauber, N. M. R. Peres, and A. K. Geim, Phys. Rev. B **78**, 085432 (2008).  
[S5] M. Jablan, H. Buljan, and M. Soljačić, Phys. Rev. B **80**, 245435 (2009).  
[S6] R. Loudon, The Quantum Theory of Light, Oxford University Press Inc., New York, 1973.  
[S7] A. O. Caldeira and A. J. Leggett, Physica A **121** 587 (1983).  
[S8] D. Banerjee, B. C. Bag, S. K. Banik, and D. S. Ray, J. Chem. Phys. **120**, 8960 (2004).  
[S9] C. Gardiner and P. Zoller, Quantum Noise: A Handbook of Markovian and Non-Markovian Quantum Stochastic Methods with Applications to Quantum Optics, Springer, Berlin, 1991.  
[S10] H.-P. Breuer and Francesco Petruccione, The Theory of Open Quantum Systems, Oxford University Press Inc., New York, 2002.  
[S11] F. Haake and R. Freibold, Phys. Rev. A **32**, 2462 (1985).  
[S12] L. Diósi, Europhys. Lett. **22**, 1 (1993).  
[S13] V. V. Dodonov, and A. V. Dodonov, J Russ Laser Res **27**, 379 (2006).  
[S14] C. A. Muschik, H. Krauter, K. Jensen, J. M. Petersen, J. I. Cirac, and E. S. Polzik, J. Phys. B: At. Mol. Opt. Phys. **45**, 124021 (2012).  
[S15] G. Giedke and J. I. Cirac, Phys. Rev. A **66**, 032316 (2002).  
[S16] C. Weedbrook, S. Pirandola, R. Garcia-Patron, N. J. Cerf, T. C. Ralph, J. H. Shapiro, and S. Lloyd, Rev. Mod. Phys. **84**, 621 (2012).  
[S17] K. Hammerer, E. S. Polzik, and J. I. Cirac, Phys. Rev. A **72**, 052313 (2005).